Virtual Reality (2004) 7: 94–102
DOI 10.1007/s10055-003-0118-5

ORIGINAL ARTICLE

Kerry L. Holland · Robert L. Williams II
Robert R. Conatser Jr. · John N. Howell
Dennis L. Cade

The implementation and evaluation of a virtual haptic back

Received: 4 July 2001 / Accepted: 27 October 2003 / Published online: 5 February 2004

Abstract A virtual haptic back (VHB) model has been developed by a cross-disciplinary team of researchers at Ohio University. Haptics give the human the sense of touch and force from virtual computer models. The objective is to create a tool for medical and related education whereby students can train in the difficult art of palpation using virtual reality before approaching human subjects. Palpation is the art of medical diagnosis through the sense of touch. Haptic anatomy could be a key area in the future of medical school training; our goal is to add science to the art of palpation to improve osteopathic, physical therapy and massage therapy training for students and practitioners. Modelling of the VHB took place in two steps. First, Cartesian back data was collected via the Metrecom Skeletal Analysis System (SAS) digitiser. The back of a prone human subject was digitised, giving an array of three-dimensional points. Several methods were considered to smooth out the back data. Spline fitting with matched first and second derivates was the chosen method. Once an acceptable graphical model was created, haptic feedback was added using the PHANToM haptic interface, allowing the human user to explore and feel the virtual back. Experienced and novice palpators formally evaluated the VHB to give us feedback for improvements. In addition, four Doctors of Osteopathy informally interacted with our model and gave verbal feedback. Our experts all suggested modelling underlying muscles and skeletal structure in addition to the skin layer for more realism. Once this is accomplished we will further program somatic dysfunction of various types in the VHB for students to diagnose. This article contributes to the state of the art in virtual haptic anatomy. While other research groups are working in this area, our work is the first specifically aimed towards osteopathic medicine, physical therapy, and massage therapy students and practitioners.

Keywords Haptics · Haptic interface · Haptics-augmented training · Virtual haptic anatomy · Virtual haptic back

K. L. Holland · R. L. Williams II (✉)
Department of Mechanical Engineering,
Ohio University, Athens, OH 45701-2979, USA
E-mail: williar4@ohio.edu
Tel.: +1-740-5931096
Fax: +1-740-5930476

R. R. Conatser Jr. · J. N. Howell
Department of Biomedical Sciences,
Ohio University, Athens, OH, USA

D. L. Cade
Department of Physical Therapy,
Ohio University, Athens, OH, USA

1 Introduction

Haptics, the science of touch, is being applied in virtual reality environments to increase realism. An example of this is virtual reality computer games that use a force-reflecting joystick.

Haptics has been applied recently to education, most notably in medical education. In the Stanford Visible Female project (Heinrichs, et al. [7], a 3D stereoscopic visualisation of the female pelvis has been developed from numerous slices of 2D pelvis data. Further, haptic feedback was enabled via the PHANToM haptic interface, allowing the user to interact with and feel the virtual model. No haptic implementation details are given in the paper. The Interventional Cardiology Training Simulator [13] links technical simulation with specific medical education content. A virtual reality-based simulator prototype for the diagnosis of prostate cancer has been developed using the PHANToM haptic interface [2]. An earlier tumor palpation VR simulation was developed by Langrana [6]. The Immersion Corporation (http://www.immersion.com) has developed haptic interfaces for injection training and sinus surgery simulation. Delingette [4] is working on realism in modelling human tissue for medical purposes. The GROPE Project [1] has developed over 30 years a 6D haptic/VR

simulation of molecular docking. The SPIDAR haptic interface has been adapted to serve as "the next generation education system" [3], although the authors do not elaborate on the type of education intended.

A group at the University of Ioannina in Greece is involved with virtual learning environments including a power glove with tactile feedback to "build a theoretical model for virtual learning environments, expanding constructivism and combining it with experiential learning" [8]. A research group at the Ohio Supercomputing Center has applied haptics in virtual environments to improve tractor safety by training young rural drivers [13]; their results show haptics increases training effectiveness. Haptics has been applied to make virtual environments accessible to blind persons [5]. Affordable haptic interfaces have been implemented to augment the teaching and learning of high school physics [13]. Also, the effectiveness of virtual reality (without haptics) has been demonstrated in the learning process [9].

The virtual haptic back (VHB) is an interdisciplinary project among three Ohio University colleges: Engineering, Osteopathic Medicine, and Health and Human Services. The purpose of the VHB is to develop a realistic haptic/graphical model of the human back that can be used for palpation in medical training. Palpation is the art of medical diagnosis through the sense of touch. Our goal is to add a component of science to the art of palpatory diagnosis. Current target applications are the diagnoses of both somatic dysfunction and movement dysfunction; we are interested in general haptic anatomy in future work.

This article presents the graphical and haptic aspects of implementing the VHB, followed by VHB evaluation by experienced and novice palpators. The major contribution of this work is as an initial step towards the big goal of creating virtual haptic anatomy for osteopathic medicine, physical therapy, and massage therapy students and practitioners.

Fig. 1 Metrecom SAS

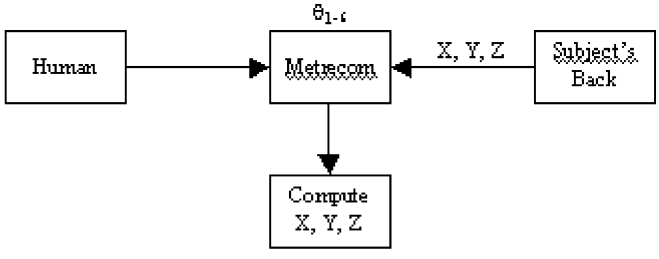

Fig. 2 Metrecom SAS flow diagram

2 Back modelling

This section presents the graphical modelling of a subject human back via measurements by the Metrecom Skeletal Analysis System (SAS), followed by our method to smooth this data for use in the VHB graphics.

2.1 The Metrecom SAS

The purpose of VHB is to train medical students in the art of palpation. With this in mind, the VHB team set out to match the model to reality as closely as possible. The back of a volunteer subject was measured using a Metrecom SAS made by Faro Technologies, Inc. (see Fig. 1).

The Metrecom SAS is a mounted electrogoniometer digitiser that reads and stores 3D position data. The electrogoniometer is a user-powered, six degree-of-freedom arm. A potentiometer is located at each pivot point. As the user moves the arm, the resistance in each potentiometer varies, resulting in a certain voltage. The computer reads these voltages, determines the corresponding joint angles and outputs a Cartesian point. The first Metrecom arm freedom is a 1-dof waist rotation about its base. The remaining arm consists of a 1-dof shoulder joint, a 1-dof elbow joint and a 3-dof wrist joint. The position sampling is time-dependent, acquiring 15 points per second.

The Metrecom SAS was developed as a measurement tool for both spinal curvature and flexibility, and joint range of motion. For our purposes, the Metrecom SAS serves solely as a 3D digitiser for a static human back. A flow diagram for the Metrecom SAS operation is pictured in Fig. 2. The human user moves the SAS pointer

over the prone subject's back, in nine horizontal strips. A computer reads the six joint angles θ_1-θ_6 and calculates the corresponding X, Y, Z locations.

2.2 Smoothing

The raw data consisted of an x, y and z array for the surface back points recorded. The time dependency of the recording resulted in an awkward spacing of the data points: they appeared to be randomly spaced as opposed to having a grid-like orientation. To remedy this, the software SigmaPlot (SPSS Science, Chicago, IL) was used to align the x, y and z arrays in a grid. Each of the nine horizontal strips of data was divided into 100 Cartesian points, resulting in 900 total data points. The data was stored as a text file and copied to Visual C++ for use in the first version of VHB. It was then copied into a Matlab program for easier manipulation. A Matlab rendering of the original data is shown in Fig. 3.

The first VHB left much, graphically and haptically, to be desired. This attempt was modelled using Ghost SDK's TriPolyMesh command (SenseAble Technologies, 1997). This allows the programmer to create a triangular mesh from the 3D data. As seen in Fig. 4, the rendering was smooth along the x-axis (i.e., horizontally), but not smooth along the y-axis (vertically). A mathematical interpretation of the data was desired, for interpolation purposes, and as a more compact and less discrete way to describe the back. As previously stated, there were nine horizontal rows of data with 100 points each (see Fig. 5). The points are located across the width of the back, starting just below the neck (T2 vertebra) and ending in the lower lumbar region (L2 vertebra).

Since the data is smooth in the x direction (left-to-right on the back), emphasis lies on smoothing the y direction (up and down the back). We determined 100 individual curve fits in the$y$ direction for smoothing purposes since each horizontal row of data contained 100 points each.

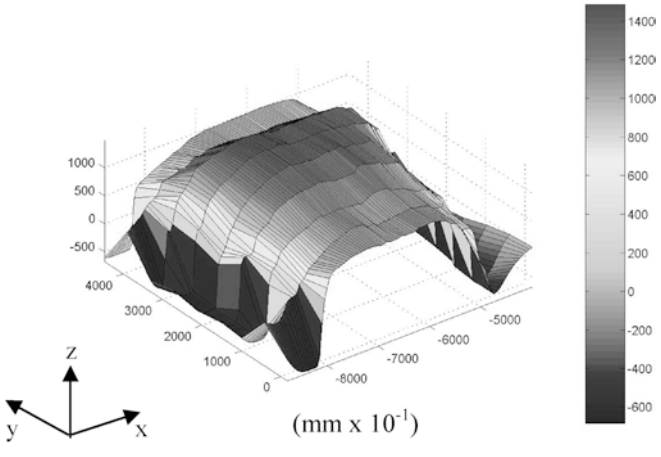

Fig. 3 A Matlab rendering of raw data VHB

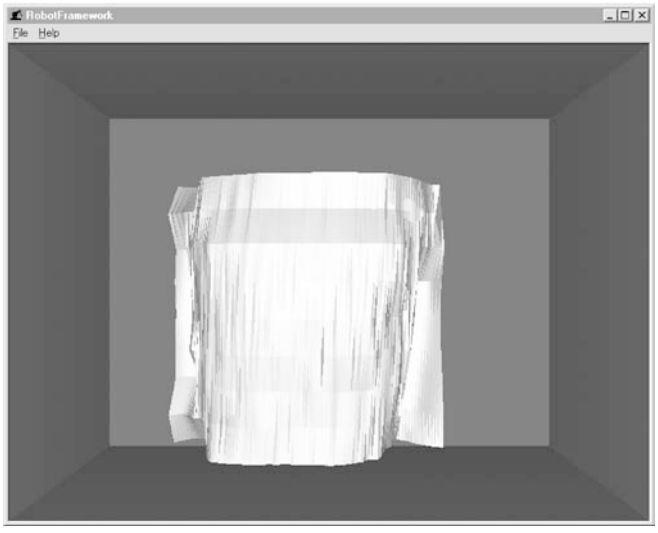

Fig. 4 A C++ view of raw data VHB

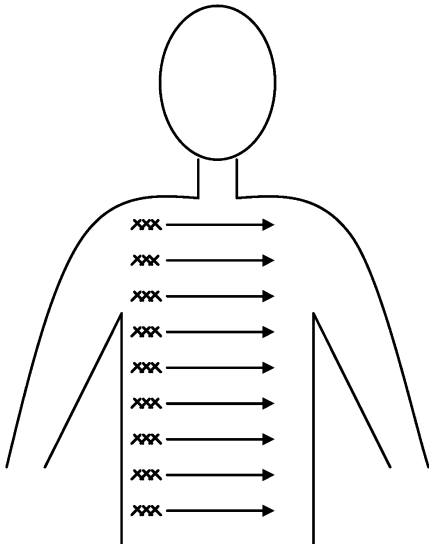

Fig. 5 Original data locations

Originally, an eighth order polynomial was applied to fit the nine data points (100 times). The curve is smooth and satisfies all data points, but dips in the upper back region, as can be seen in Fig. 6. The data points in Figs. 6, 7 and 8 correspond to the y direction up and down the back; the left-most point is measured at the L2 vertebra and the right-most point is measured at the T2 vertebra.

To fix the dip problem of Fig. 6, three separate curve fits were generated to fit the back. The middle curve was a quartic polynomial to fit point three through point seven of the original eighth order curve. The first and third curves used the first three and last three data points, respectively, to generate quadratic curves. The endpoints of the middle section are reused in order to connect each curve with its predecessor. The results of this method are shown in Fig. 7.

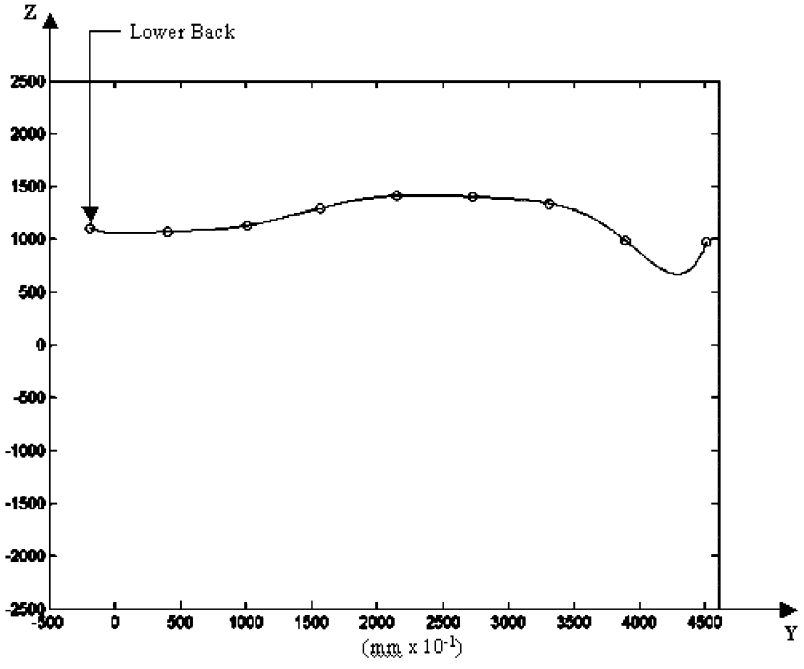

Fig. 6 Eighth order curve fit

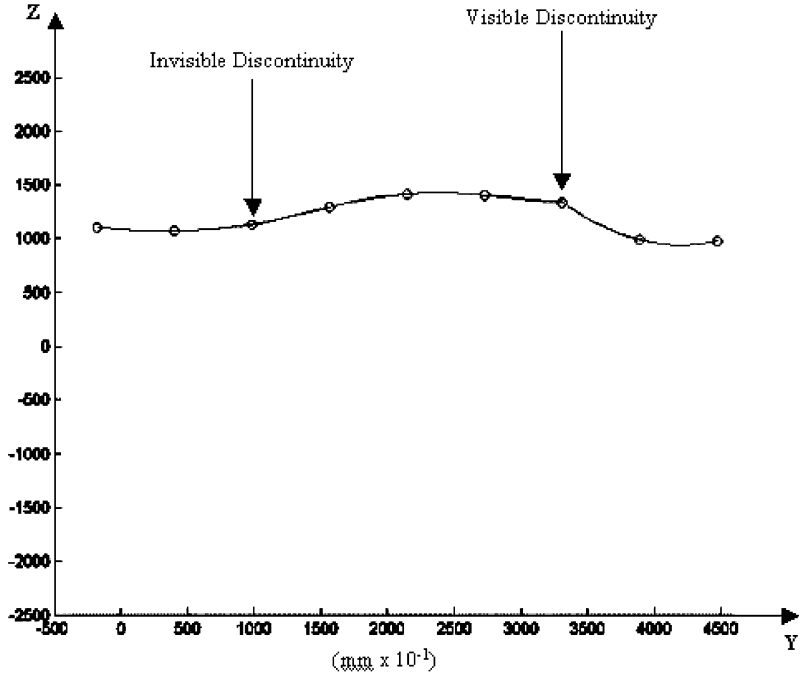

Fig. 7 Three separate curve fits

In Fig. 7 it is clear that the three separate curve fits result in a visible discontinuity (the lower back discontinuity is not as visible). Therefore, we chose to match the three polynomials at their junction points not only in position but also matching their first and second derivatives across the two junction points. With the additional derivative matching constraints, the first and third polynomials must be of third order, and the middle polynomial is increased to sixth order. This will not only smooth the back in the$y$ direction and include all the original data points, but it will create a smooth transition between the three different curves (see Fig. 8). Eqs. 1, 2 and 3 represent the three curves plotted in Fig. 8:

$$z_A(y) = a_1 + b_1 y + c_1 y^2 + d_1 y^3 \quad (1)$$

$$z_B(y) = a_2 + b_2 y + c_2 y^2 + d_2 y^3 + e_2 y^4 + f_2 y^5 + g_2 y^6 \quad (2)$$

$$z_C(y) = a_3 + b_3 y + c_3 y^2 + d_3 y^3 \quad (3)$$

where $z_A(y)$, $z_B(y)$, and $z_C(y)$ are the three polynomials, a_{1-3},b_{1-3},b_{1-3},d_{1-3},e_2,f_2 and g_2 are the unknowns, and y is

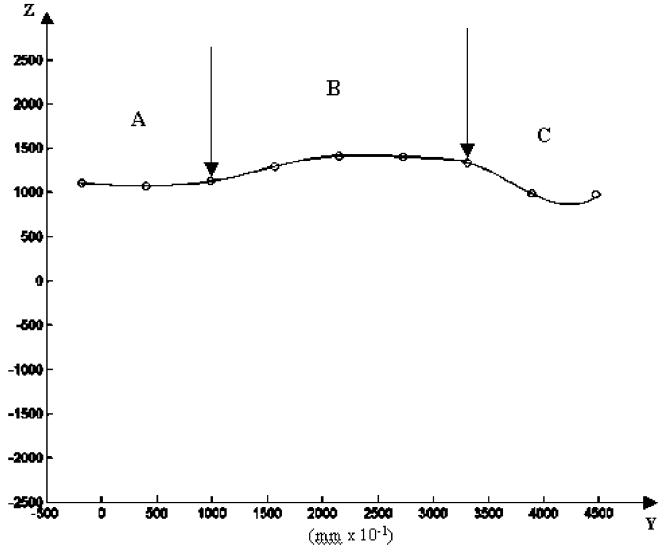

Fig. 8 Matching first and second derivatives

the independent variable. Eqs. 1 and 3 are third order, and 2 is sixth order, chosen to match the number of polynomial constants with the number of given constraints. Four constants from Eq. 1, seven constants from Eq. 2 and four constants from Eq. 3 match the fifteen constraints, discussed next.Each of the position data points must lie on the curve: three for the first curve, five for the second curve and three for the third curve. To fix the discontinuity seen in Fig. 7, we force both the first derivatives and second derivatives to match for different polynomials meeting at the two junctions. The constraints are listed below with $y_{1–9}$ and $z_{1–9}$ representing the data points and $a_{1–3}$,$b_{1–3}$,$c_{1–3}$,$d_{1–3}$, e_2,f_2 and g_2 are the constants to be determined for each of the three polynomials. Eqs. 4, 5, 6, 7, 8, 9, 10, 11, 12, 13 and 14 are position constraints, Eqs. 15 and 16 match the first derivatives, and Eqs. 17 and 18 match the second derivatives.

$$z_1 = a_1 + b_1y_1 + c_1y_1^2 + d_1y_1^3 \tag{4}$$

$$z_2 = a_1 + b_1y_2 + c_1y_2^2 + d_1y_2^3 \tag{5}$$

$$z_3 = a_1 + b_1y_3 + c_1y_3^2 + d_1y_3^3 \tag{6}$$

$$z_3 = a_2 + b_2y_3 + c_2y_3^2 + d_2y_3^3 + e_2y_3^4 + f_2y_3^5 + g_2y_3^6 \tag{7}$$

$$z_4 = a_2 + b_2y_4 + c_2y_4^2 + d_2y_4^3 + e_2y_4^4 + f_2y_4^5 + g_2y_4^6 \tag{8}$$

$$z_5 = a_2 + b_2y_5 + c_2y_5^2 + d_2y_5^3 + e_2y_5^4 + f_2y_5^5 + g_2y_5^6 \tag{9}$$

$$z_6 = a_2 + b_2y_6 + c_2y_6^2 + d_2y_6^3 + e_2y_6^4 + f_2y_6^5 + g_2y_6^6 \tag{10}$$

$$z_7 = a_2 + b_2y_7 + c_2y_7^2 + d_2y_7^3 + e_2y_7^4 + f_2y_7^5 + g_2y_7^6 \tag{11}$$

$$z_7 = a_3 + b_3y_7 + c_3y_7^2 + d_3y_7^3 \tag{12}$$

$$z_8 = a_3 + b_3y_8 + c_3y_8^2 + d_3y_8^3 \tag{13}$$

$$z_9 = a_3 + b_3y_9 + c_3y_9^2 + d_3y_9^3 \tag{14}$$

$$b_1 + 2c_1y_3 + 3d_1y_3^2 = b_2 + 2c_2y_3 + 3d_2y_3^2 + 4e_2y_3^3 + 5f_2y_3^4 + 6g_2y_3^5 \tag{15}$$

$$b_3 + 2c_3y_7 + 3d_3y_7^2 = b_2 + 2c_2y_7 + 3d_2y_7^2 + 4e_2y_7^3 + 5f_2y_7^4 + 6g_2y_7^5 \tag{16}$$

$$2c_1 + 6d_1y_3 = 2c_2 + 6d_2y_3 + 12e_2y_3^2 + 20f_2y_3^3 + 30g_2y_3^4 \tag{17}$$

$$2c_3 + 6d_3y_7 = 2c_2 + 6d_2y_7 + 12e_2y_7^2 + 20f_2y_7^3 + 30g_2y_7^4 \tag{18}$$

Eqs. 4, 5, 6, 7, 8, 9, 10, 11, 12, 13, 14, 15, 16, 17 and 18 were written in matrix/vector form (Eq. 19) and the unknown polynomial coefficients ($a_{1–3}$, $b_{1–3}$, $c_{1–3}$, $d_{1–3}$, e_2, f_2, and g_2) were solved from this set of 15 linear equations in 15 unknowns.

$$\begin{bmatrix}
1 & y_1 & y_1^2 & y_1^3 & 0 & 0 & 0 & 0 & 0 & 0 & 0 & 0 & 0 & 0 & 0 \\
1 & y_2 & y_2^2 & y_2^3 & 0 & 0 & 0 & 0 & 0 & 0 & 0 & 0 & 0 & 0 & 0 \\
1 & y_3 & y_3^2 & y_3^3 & 0 & 0 & 0 & 0 & 0 & 0 & 0 & 0 & 0 & 0 & 0 \\
0 & 0 & 0 & 0 & 1 & y_3 & y_3^2 & y_3^3 & y_3^4 & y_3^5 & y_3^6 & 0 & 0 & 0 & 0 \\
0 & 0 & 0 & 0 & 1 & y_4 & y_4^2 & y_4^3 & y_4^4 & y_4^5 & y_4^6 & 0 & 0 & 0 & 0 \\
0 & 0 & 0 & 0 & 1 & y_5 & y_5^2 & y_5^3 & y_5^4 & y_5^5 & y_5^6 & 0 & 0 & 0 & 0 \\
0 & 0 & 0 & 0 & 1 & y_6 & y_6^2 & y_6^3 & y_6^4 & y_6^5 & y_6^6 & 0 & 0 & 0 & 0 \\
0 & 0 & 0 & 0 & 1 & y_7 & y_7^2 & y_7^3 & y_7^4 & y_7^5 & y_7^6 & 0 & 0 & 0 & 0 \\
0 & 0 & 0 & 0 & 0 & 0 & 0 & 0 & 0 & 0 & 0 & 1 & y_7 & y_7^2 & y_7^3 \\
0 & 0 & 0 & 0 & 0 & 0 & 0 & 0 & 0 & 0 & 0 & 1 & y_8 & y_8^2 & y_8^3 \\
0 & 0 & 0 & 0 & 0 & 0 & 0 & 0 & 0 & 0 & 0 & 1 & y_9 & y_9^2 & y_9^3 \\
0 & -1 & -2y_3 & -3y_3^2 & 0 & 1 & 2y_3 & 3y_3^2 & 4y_3^3 & 5y_3^4 & 6y_3^5 & 0 & 0 & 0 & 0 \\
0 & 0 & 0 & 0 & 0 & 1 & 2y_7 & 3y_7^2 & 4y_7^3 & 5y_7^4 & 6y_7^5 & 0 & -1 & -2y_7 & -3y_7^2 \\
0 & 0 & -2 & -6y_3 & 0 & 0 & 2 & 6y_3 & 12y_3^2 & 20y_3^3 & 30y_3^4 & 0 & 0 & 0 & 0 \\
0 & 0 & 0 & 0 & 0 & 0 & 2 & 6y_7 & 12y_7^2 & 20y_7^3 & 30y_7^4 & 0 & 0 & -2 & -6y_y
\end{bmatrix}
\begin{Bmatrix} a_1 \\ b_1 \\ c_1 \\ d_1 \\ a_2 \\ b_2 \\ c_2 \\ d_2 \\ e_2 \\ f_2 \\ g_2 \\ a_3 \\ b_3 \\ c_3 \\ d_3 \end{Bmatrix}
=
\begin{Bmatrix} z_1 \\ z_2 \\ z_3 \\ z_3 \\ z_4 \\ z_5 \\ z_6 \\ z_7 \\ z_7 \\ z_8 \\ z_9 \\ 0 \\ 0 \\ 0 \\ 0 \end{Bmatrix} \tag{19}$$

Eq. 19 was solved for each of the 100 strips of data to obtain the individual curves for the 100 vertical sections of the back. The final Matlab rendering is Fig. 9.

The rendering in Visual C++ is shown in Fig. 10. The discontinuous data due to unsteady measurement along the sides of the back has been eliminated between Figs. 9 and 10.

At this point a discussion on errors in our back model is warranted. Firstly, in the lab it is impossible to measure the human back so quickly such that the subject can survive on one breath of air. That is, the natural breathing of the human subject caused some error in our raw data measurements. We don't know how to quantify this error, but one can imagine the worst error case simply by breathing and registering the maximum displacement of the human back and chest. This error will be different for different subjects. Secondly, additional errors can be introduced by our data smoothing techniques presented above, accomplished to improve the graphics and haptics qualities of our model. Since we force the original data points to be met, we believe this source of error is bounded by the more significant case of the breathing error. In any case, the (unknown) errors introduced do not pose a problem in our project since our aim is not to model a specific human back with high accuracy but rather to model a reasonable, generic human back for training purposes.

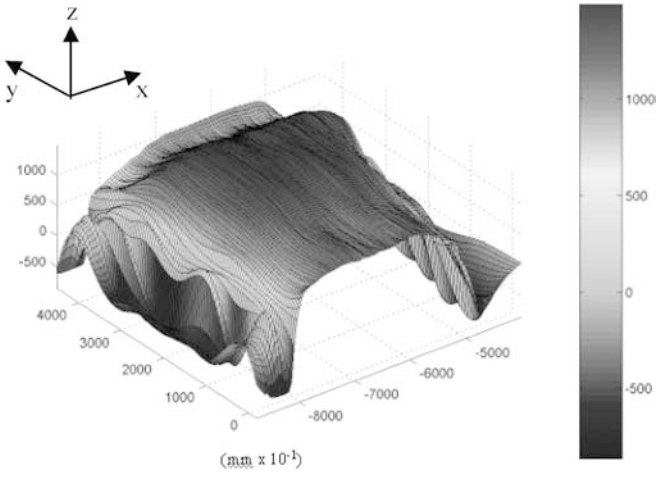

Fig. 9 Matlab rendering of final data

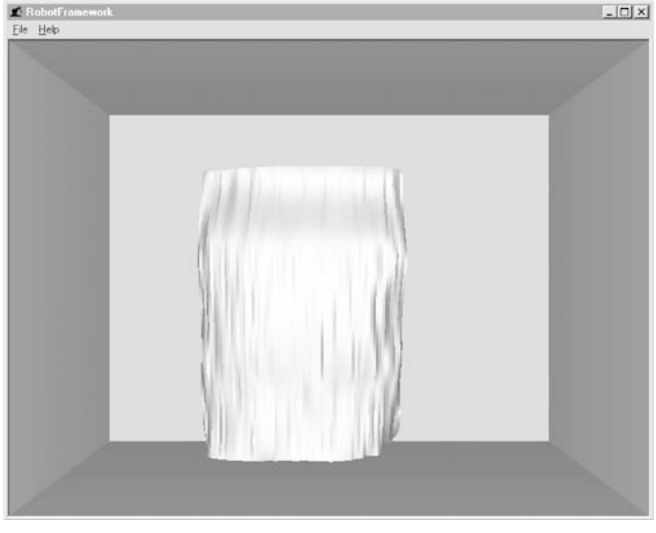

Fig. 10 A C++ rendering of final data VHB

3 VHB implementation

This section presents an implementation of the VHB in virtual reality using the PHANToM haptic interface and graphics and haptics programming.

3.1 PHANToM haptic interface

The PHANToM haptic interface (Fig. 11) developed by SenseAble Technologies, Inc. operates like the Metrecom SAS but does more than yield Cartesian points. It uses the calculated position information to determine what forces to relay back to the user via its three motors. A flow diagram for the PHANToM is pictured in Fig. 12. The human finger moves the PHANToM to desired X, Y, Z Cartesian locations (sensed internally via joint encoders $\theta_1,\theta_2,\theta_3$); this Cartesian input is sent to a virtual computer model. The haptic/graphical software determines what Cartesian force vector F_X,F_Y,F_Z the human should feel and the PHANToM generates this force at the human finger (accomplished internally via joint torques τ_1,τ_2,τ_3).

3.2 Graphics and haptics programming

The first step in modelling the VHB using Ghost SDK (the software used to program the PHANToM, developed by SenseAble Technologies Inc., 1997), is to define what is included in the haptic scene. The Ghost SDK uses OpenGL for 3D graphics. A pointer to the root of the desired scene graph is defined, and the haptic simulation is performed by a servo loop operating at a rate

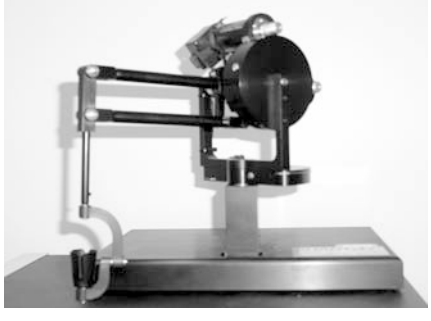

Fig. 11 The PHANToM haptic interface

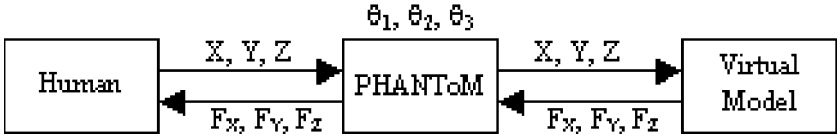

Fig. 12 The PHANToM flow diagram

of 1 kHz. The servo loop performs the following functions: 1) update the PHANToM node position in the scene graph, 2) update the dynamic state of all dynamic objects, 3) detect collisions between PHANToM nodes and geometric nodes in the scene graph, and 4) send resultant forces back to the PHANToM.

The VHB makes use of GHOST SDK's gstTriPolyMesh command to define the back. The VHB position data is defined as three arrays (x, y and z) in a header file. The inputs to gstTriPolyMesh are: 1) the number of total data points, 2) the position data, 3) the number of triangles in the mesh, and 4) the three points of each triangle in the mesh. The VHB workspace is contained using Ghost's gstBoundaryCube function, which confines the user's movement to a box shaped volume.

The haptic feedback is based on linear springs, normal to the surface of each triangle in the mesh. The spring constant is the same over the entire back, set for a reasonable feel. Part of our future work plans are to measure and implement a more realistic, nonlinear human tissue model (as in [4]), including subcutaneous soft tissues and skeletal elements. These additional layers will be implemented in the VHB using force thresholds with the PHANToM.

4 VHB evaluation results

This section presents the results of our preliminary VHB evaluation study to measure project results and give us a basis for future improvements.

A significant improvement between the raw VHB and the smoothed VHB is both visible and palpable. The most significant improvement is in the vertical direction. In the C++ rendering of the raw data, the nine horizontal sample strips were visible and palpable (Fig. 4). The smoothing method of choice (curve fitting with matched derivatives vertically down the back) resulted in interpolated data. Since each strip of interpolated data was independent of the strip beside it, variance in the z-direction occurred at certain widthwise sections of the back. These vertical strips are visible in the final C++ rendering of the back (Fig. 10).

The evaluators were asked to rate both raw and smoothed versions of the VHB in the following categories: colour, shading, graphic and haptic smoothness, graphic and haptic contour, stiffness, friction, and real-time interaction. They were asked to evaluate the VHB in each category on a scale of one (very unrealistic) to ten (very realistic). All of these performance measures were subjective, based on evaluator opinions; we have no method to objectively measure results in any of these categories.

Six experienced palpators and twenty novice palpators evaluated the VHB. All experienced palpators came from the the Ohio University School of Physical Therapy. They were second year graduate students who had acquired standard palpations skills through practice and schooling. Any person inexperienced in the art of palpation was considered a novice. All novices for this experiment were students from the Ohio University College of Engineering. This study was not intended for statistical significance, rather as an initial evaluation to give us areas for future improvement of our model. We wished to have more subjects, but six experienced palpators was all we could arrange in the project time frame.

Evaluation sheets were given along with a brief explanation of the VHB project. Brief PHANToM training was provided. Evaluators were given two evaluation sheets and instructed how to complete them, one for the raw VHB and one for the final VHB. General comments were strongly encouraged. Finally, the user was presented with both models, raw VHB first. Average results for both groups on both versions of the VHB are in Table 1; Table 2 gives the associated standard deviations.

On average, experienced palpators rated raw VHB graphics 15.7% higher than novices. However, experienced palpators rated raw VHB haptics 8.4% lower than novices, due to their palpation expertise. High standard deviations resulted, varying from 1.25 to 3.02 on a scale of 10. This could be due to a lack of experience using the PHANToM. None of the six experienced palpators had used the PHANToM before. Although they were briefly instructed, a few subjects commented that the device was hard to adapt to. This is not uncommon: past non-VHB demonstrations have resulted in similar comments.

In all categories (graphic and haptic), both groups rated the smoothed VHB as improved (with the exception of real-time interaction for the experienced palpators).

Table 1 Raw and final VHB averages

	Novice Raw	Novice Final	Experienced Raw	Experienced Final
Graphics				
Colour	5.90	7.10	6.50	7.33
Smoothness	4.40	6.75	5.50	6.50
Shading	5.70	7.35	6.58	6.60
Contour	5.25	6.95	6.00	6.67
Haptics				
Smoothness	5.05	7.00	6.17	6.50
Stiffness	6.40	7.25	5.00	6.17
Friction	5.95	7.45	5.33	5.50
Contour	6.25	7.70	5.17	5.33
Real-time interaction	8.00	8.20	9.00	8.83

Table 2 Raw and final VHB standard deviations

	Novice Raw	Novice Final	Experienced Raw	Experienced Final
Graphics				
Colour	1.74	1.37	2.26	2.25
Smoothness	2.26	1.52	2.59	3.08
Shading	1.81	1.39	2.25	2.51
Contour	2.07	1.90	2.61	2.58
Haptics				
Smoothness	2.28	1.75	1.47	2.07
Stiffness	1.39	1.25	2.53	2.64
Friction	2.24	1.28	3.01	3.02
Contour	2.31	1.75	2.79	3.08
Real-time interaction	2.15	1.44	0.63	0.75

Table 3 Percent improvements from raw to final VHB

	Novice (%)	Experienced (%)
Graphics		
Colour	20.3	12.8
Smoothness	53.4	18.2
Shading	28.9	0.3
Contour	32.4	11.2
Haptics		
Smoothness	38.6	5.3
Stiffness	13.3	23.4
Friction	25.2	3.2
Contour	23.2	3.1
Real-time interaction	2.5	–1.9

Relatively speaking, the novice group rated the second version of VHB much more improved than did the experienced palpators. The percent differences in the averages for each category rated by both groups are shown in Table 3.

Both positive and negative feedback was given in the comments. Experienced palpators were more likely to make a comment, and were more detailed. As seen from the abovementioned tables, virtually all marks improved for the final, smoothed VHB. The fundamental theme in most comments was that the back must be modelled considering the underlying muscle and bone structure to help the VHB feel like an actual human back.

Now, the fact that the final, smoothed VHB is preferable to the raw version is not surprising. In fact, we would not consider using the raw VHB in the future just based on the modelling team's opinions and experience with the models. Again, the evaluation study was not intended to be statistically significant, but it was simply intended to improve our model in future work. The comments from evaluators, especially from our experienced subjects and doctors (see below) were the most valuable results from our evaluation study.

More sophisticated and long-term suggestions were offered by practicing osteopathic doctors with tactile specialties (four Doctors of Osteopathy (DOs) independently tested the raw and final VHB models, though they did not fill in a formal evaluation). The DOs also suggested programming haptic tissue and skeleton beneath the skin. Since the digitising of a skeleton is not trivial, two of the DOs independently suggested programming different sized spheres to represent the spinous and transverse processes of the human spine. This eliminates the programming of parts of the skeleton that the palpator cannot ordinarily feel. This type of haptic modelling would enable the programming of different types of somatic dysfunction. Another suggestion to aid in palpation training was to turn off the graphical clues for different types of dysfunction, thus testing the student's ability to diagnose by feel.

5 Conclusions

This article has presented implementation and evaluation of the VHB by an interdisciplinary team of researchers and educators at Ohio University. We are involved in virtual haptic anatomy, specifically for the purpose of providing a tool for students in medical and related fields to better train themselves in the art of palpatory diagnosis. Since the human sense of touch is generally less-developed than vision and hearing, we wish to add a component of science to the art of palpatory diagnosis, both in learning and practice.

The first-cut VHB has been implemented in virtual reality using a PHANToM haptic interface. The back model was measured, the position data was smoothed and haptic feedback was added. We have concluded initial VHB evaluation by experienced and novice palpators.

Based on the VHB project evaluation, we will next add muscle and skeletal structure layers for the trainee to feel under the existing skin layer. This will require the development of a more advanced haptics model. We will then program various types of somatic dysfunction for students in various palpatory disciplines to practice their diagnoses. This next phase will conclude with an evaluation to ensure that project results meet the needs of students, professors, doctors and other practitioners.

Some other research groups are involved in virtual haptic anatomy. The major contribution of this article is our focus on osteopathic medicine, physical therapy, and massage therapy students and practitioners. No previous research group has taken this focus to date, according to our literature search.

References

1. Brooks Jr FP, Ming OY, Batter JJ and Kilpatrick PJ (1990) Project GROPE: haptic displays for scientific visualization. Comp Graph 24(4):177–185
2. Burdea G, Patounakis G and Popescu V (1999) Virtual reality-based training for the diagnosis of prostate cancer. IEEE Trans Biomed Engin 46(10):1253–60
3. Cai Y, Wang S and Sato M (1997) Human-scale direct motion instruction system device for education systems. IEICE Trans Info Sys E80-D(2):212–217
4. Delingette H (1998) Toward realistic soft-tissue modeling in medical simulation. Proceedings of the IEEE 86(3):512–523

5. Jansson G, Petrie H, Colwell C, Kornbrot D, Fänger J, König H, Billberger K, Hardwick A and Furner S (1999) Haptic virtual environments for blind people: exploratory experiments with two devices. International Journal of Virtual Reality, 4(1)10–20
6. Langrana N (1997) Human performance using virtual reality tumor palpation simulation. Comp Graph 21(4):451–458
7. Heinrichs WL, Srivastava S, Brown J, Latombe J-C, Montgomery K, Temkin B and Dev P (2000) A steroscopic palpable and deformable model: Lucy 2.5. In: Proceedings of the Third Visible Human Conference, Bethesda, MD, 5–6 October 2000
8. Mikropoulos TA, Nikolou E (1996) A virtual hand with tactile feedback for virtual learning environments. In: Proceedings of the World Conference on Educational Multimedia and Hypermedia, Boston, MA, 17–22 June 1996
9. North SM (1996) Effectiveness of virtual reality in the motivational processes of learners. International Journal of Virtual Reality 2(1):17–21
10. SenseAble Technologies (1997) Ghost SDK Programmer's Guide Version 3.0, SenseAble Technologies Inc., Woburn, MA
11. Shaffer D, Meglan D, Ferrell M and Dawson S (1999) Virtual rounds: simulation-based education in procedural medicine. In: Proceedings of the 1999 SPIE Battlefield Biomedical Technologies Conference, Orlando, FL 3712:99–108
12. Stredney D, Wiet GJ, Yagel R, Sessanna D, Kurzion Y, Fontana M, Shareef N, Levin M, Martin K and Okamura A (1998) A comparative analysis of integrating visual representations with haptic displays. In: Proceedings of MMVR6, San Diego, CA, January 1998
13. Williams II RL, Chen M-Y and Seaton JM (2001) Haptics-augmented high school physics tutorials. International Journal of Virtual Reality 5(1)